Available online at www.sciencedirect.com
SCIENCE DIRECT®
ELSEVIER
Journal of Nuclear Materials 337–339 (2005) 490–494
journal of nuclear materials
www.elsevier.com/locate/jnucmat

Analysis of the Dα spectral line shape on the carbon limiter insertion experiments in Heliotron J

H. Kawazome [a,*], K. Takahashi [a], S. Tsuboi [a], H. Arimoto [a], T. Mizuuchi [b], N. Nishino [c], H. Okada [b], K. Nagasaki [b], S. Kobayashi [b], S. Yamamoto [b], Y. Suzuki [a], K. Ohashi [a], S. Nakazawa [a], M. Kaneko [a], H. Shidara [a], Y. Fukagawa [a], S. Nishio [a], M. Yamada [a], H. Yamazaki [a], K. Kondo [a], F. Sano [b]

[a] *Graduate School of Energy Science, Kyoto University, Gokasho, Uji Kyoto 611-0011, Japan*
[b] *Institute of Advanced Energy, Kyoto University, Gokasho, Uji Kyoto 611-0011, Japan*
[c] *Graduate School of Engineering, Hiroshima University, Higashi-Hiroshima, Hiroshima 739-8527, Japan*

Abstract

In order to investigate the velocity distribution function of deuterium atoms, which gives information about the recycling process, in the Heliotron J edge plasma region, spectral line shapes of Dα emitted in front of a carbon limiter have been measured with a high-resolution spectrometer. Measured spectral profiles have an asymmetric structure and are decomposed into the broad and narrow Gaussian components. The central wavelengths of each component shift toward the blue side. The intensity distribution is similar to the footprint of the magnetic field lines on the limiter surface. The emission from reflected atoms affects the intensity distribution of the broad component.

PACS: 52.40.−w; 52.40.Hf
Keywords: Heliotron J; Hydrogen atoms; Limiter; Spectroscopy

1. Introduction

In order to control fuelling, pumping and impurity generation in fusion plasmas, understanding the behavior of neutral deuterium (hydrogen) atoms in the edge and divertor region is necessary. The essential parameters for understanding their behavior are the velocity distribution and flow velocity. Knowledge of the velocity distribution determines the penetration depth of the neutral atoms and gives information about the recycling process. The velocity distribution of the deuterium atoms is composed of low and high energy components. The low energy component is due to molecular dissociation and ionization. The high energy component is the contribution of the reflected atoms and the atoms produced by the charge exchange reaction. A detailed analysis of spectral profiles of Dα provides information on the behavior of neutral deuterium atoms. High-resolution spectroscopic measurements are very powerful methods and performed in many magnetically confined devices [1–6]. In this paper, behavior of the deuterium atoms in front of a carbon limiter has been investigated

* Corresponding author. Tel.: +81 774 38 4442; fax: +81 774 32 9397.
E-mail address: kawazome@center.iae.kyoto-u.ac.jp (H. Kawazome).

0022-3115/$ - see front matter © 2004 Elsevier B.V. All rights reserved.
doi:10.1016/j.jnucmat.2004.09.046

by a spectroscopic method in Heliotron J. Heliotron J is a medium-size helical axis Heliotron with $l = 1$ and $m = 4$, which can form various magnetic configurations by changing the current combinations of the coil set [7]. Realization of helical and island diverter configurations is one of the main objectives [8–10]. For realization of these configurations, it is important to understand the recycling process at the edge plasma region, which has the complex magnetic field structure unique to the Heliotron J device.

2. Experimental setup

Fig. 1 shows a schematic drawing of the experimental setup for the carbon limiter insertion. The carbon limiter is inserted from the bottom of the torus into the edge plasma region. The diameter of the limiter head is 90 mm. The insert position is identified by the distance from the equatorial plane of the torus, denoted by z, and the last closed flux surface (LCFS) is $z = -175$ mm in the standard configuration [11]. In the experiments, the limiter is inserted at the position of $z = -200$ mm. The edge electron density and temperature are measured with a Langmuir probe located on the top of the limiter. A two-dimensional optical fiber array is used for the spectroscopic measurement. The arrangement of the array is 10×3. For the observation from the top port, the viewing area is 57 mm in the major radius direction and 255 mm in the toroidal direction. The spot size and distance between adjacent spots are about 6 mm and 14 mm, respectively, in front of the limiter. For the observation from the side port, the viewing area is 33 mm in the toroidal direction and 100 mm in the Z-direction. The diameter and distance between adjacent spots are about 2.2 mm and 11 mm, respectively. Fig. 2 shows a schematic drawing of the limiter and projection of viewing area for the observation from the side port. The spectrometer is a 1.26 m Czerny–Turner type with an 1800 lines/mm holographic grating. The space- and time-resolved spectral profiles are detected with a charge-coupled device and 22 sight lines are selected for simultaneous measurements. The minimum time resolution is 20 ms. The absolute wavelength is calibrated with H_2 and D_2 lamps, and the reciprocal linear dispersion is obtained as 0.0049 nm/pixel at around 656.0 nm. The minimum detectable velocity of the deuterium atom is 2.2×10^3 m/s.

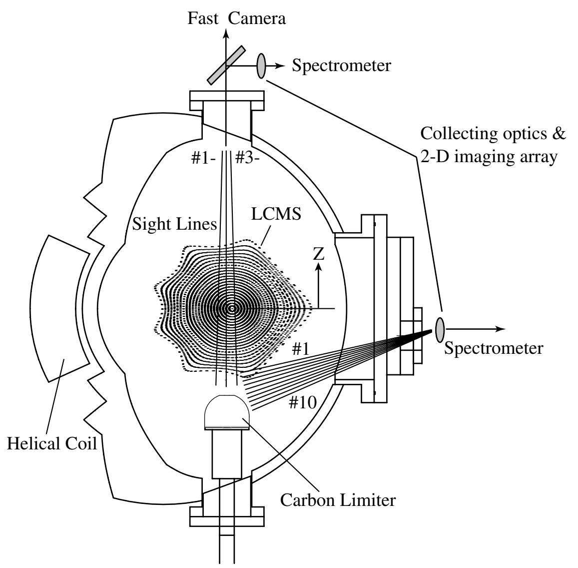

Fig. 1. The schematic drawing of the experimental setup of the carbon limiter insertion. The magnetic surface corresponds to that of the standard configuration. The position of the limiter is identified by the distance from the equatorial plane of the tours, denoted by z, and the LCFS is $z = -175$ mm.

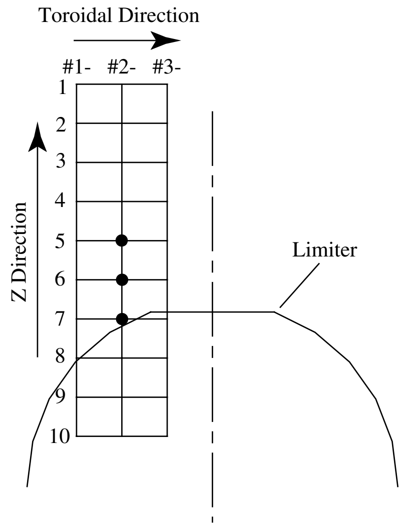

Fig. 2. The schematic drawings of the limiter and projection of the viewing area by the two-dimensional optical fiber array for observation from the side port. Closed circles are correspond to the spot size.

3. Results and discussion

The Dα spectral profiles emitted in front of the carbon limiter are measured in 70 GHz ECH plasmas. The plasmas are produced in the standard configuration and the pulse duration is 100 ms. The gas puffing is controlled to keep the electron density almost constant during the discharge. Fig. 3 shows the Dα spectral profile measured from the top port. The slit width is 30 μm and the sight line is #2–5. The spectral profile has an

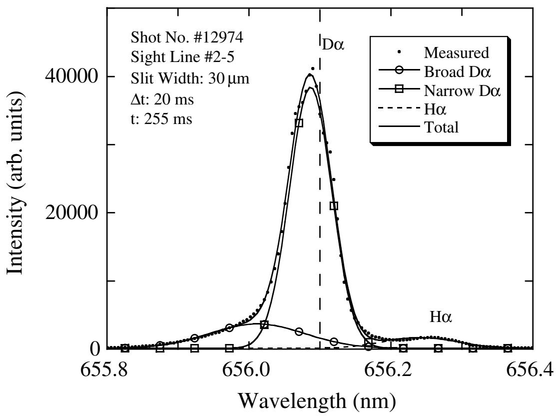

Fig. 3. The Dα spectral profile emitted in front of the carbon limiter and measured from the top port. The spectral profile has an asymmetric structure and can be decomposed into three Gaussian components. The Dα line is fitted a sum of two components, broad and narrow. The Hα line is fitted by a single component.

asymmetric structure and can be decomposed into three Gaussian components. Since deuterium atoms have mainly two components, cold and warm, at the edge plasma region, it is necessary to consider the sum of two components. But as can be seen in the figure, the intensity of the Hα line is smaller than that of the Dα line and is too weak to be treated as a composition of two components. In the Dα spectral profile, the central wavelengths of each component shift toward the blue side. The flow velocities corresponding to the shifts are 4.6×10^4 m/s and 6.2×10^3 m/s in the broad and narrow components, respectively.The errors caused by the fitting process are less than 1.8×10^3 m/s. The energy of clearly distinguished shoulder in the blue wing ranges from 26 eV to 147 eV. The half widths of the broad and narrow components are equal to the Doppler widths of deuterium atoms at the temperatures of 19.6 eV and 3.5 eV, respectively. It seems that the broad component is due to the emission from charge exchanged and reflected atoms and that the narrow component is due to the emission from dissociated atoms.

From a calculated result of the footprint of the magnetic field lines on the limiter surface, the sight line #2–5 is viewing an area in which strike points of the magnetic field line are concentrated. Most of the emission attributed to the reflected atoms is distributed in the blue side because the reflected atoms move away from the limiter surface and most of them move towards the spectrometer. For the spectral profile shown in Fig. 3, we estimate the trajectory of the reflected atoms produced by the D^+ reflection on the limiter. Based on the calculated result for the footprint on the limiter surface, the incident angle of the ion flux is selected as 85°. The incident energy of the flux is approximately 80 eV because of the sheath acceleration for $T_e^{edge} = 20$ eV [12,13]. In front of the limiter, the ion temperature is assumed to be equal to the electron temperature, and we obtain the velocity of reflected atoms to be 8.5×10^4 m/s [14]. Since the velocity estimated from the shift of the central wavelength is 4.6×10^4 m/s, the angle between the sight line #2–5 and the trajectory of the reflected atoms is estimated to be about 123°. In this case, the reflection angle is 75°. For detailed discussion about the angular distribution of the reflected atoms, numerical calculations with Monte Carlo method are required. However, the estimated reflection angle is consistent with the characteristic of the calculated angular distribution [15]. The shift of the central wavelength of the broad component is mainly due to the emission from the reflected atoms.

Fig. 4 shows the dependence of the intensity of the broad component on the edge electron density for the sight line #2–3, #2–5 and #2–8. The intensities increase with the edge electron density. The intensity measured at the sight line #2–5 has a maximum value and largest rate of increase. The sight line #2–5 is viewing strike points of the divertor legs. The connection length of the divertor legs is about 80 m. On the other hand, intensities of the sight line #2–3 and #2–8 have a similar rate of increase. Since the emission due to reflected atoms has a large contribution to the intensity of the broad component, it is our expectation that the broad component intensity will increase with the particle flux coming to the limiter surface. In the measurement, the edge electron temperature is almost constant ($T_e^{edge} \simeq 20$ eV) with changes in edge electron density. Thus incident energies of the deuterium ion flux caused by the sheath acceleration also remain constant. The ion flux estimated from the ion saturation current linearly increases with the

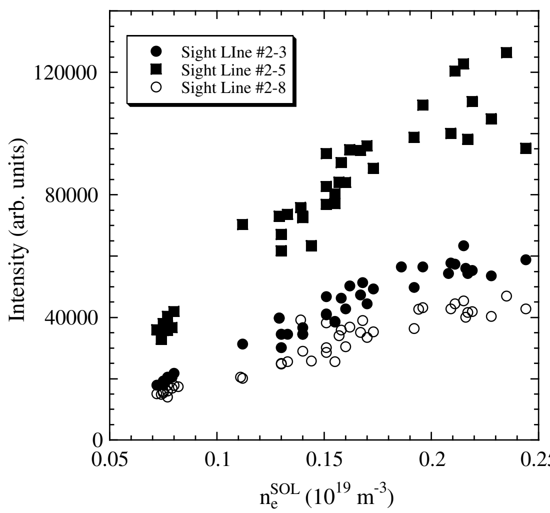

Fig. 4. Dependence of the broad component intensity on the edge electron density for the sight lines #2–3, #2–5 and #2–8.

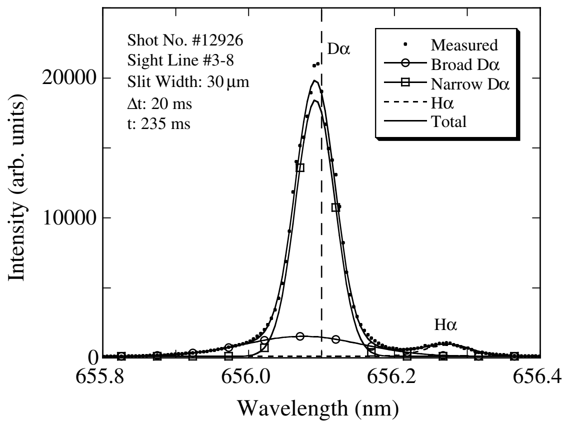

Fig. 5. The Dα spectral profile measured from the side port. The spectral profile has an asymmetric structure and can be decomposed into the three components.

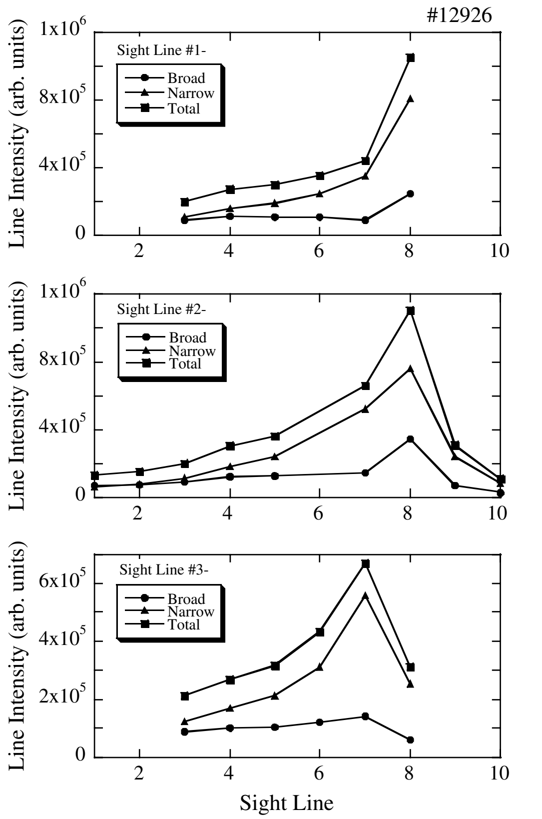

Fig. 6. The distribution of the line intensities of the Dα emissions as measured from the side port.

edge electron density because the edge electron temperature does not change. In Fig. 4, the intensities of the broad component are in proportion to the edge electron density. This result indicates that the increase in the intensity of the broad component is caused by an increase of the incident ion flux.

The Dα spectral profile, measured from the side port, is decomposed into the three components and shown in Fig. 5. The flow velocities of the broad and narrow components of Dα line are 9.1×10^3 m/s and 4.6×10^3 m/s, respectively. For the reflected atoms, the velocity component toward the outside of the torus is one order magnitude smaller than that toward the Z-direction. Fig. 6 shows the distribution of the line intensities of the broad and narrow components at the measurement from the side port. For each row of the two dimensional imaging fiber, the sight lines having the maximum intensity view around the limiter head as shown in Fig. 2. Intensities decrease exponentially, and the decay length of the intensity for each sight line is about 40 mm.

4. Summary

The carbon limiter has been inserted into the Heliotron J edge plasmas and the spectral line profiles of Dα emitted in front of the limiter have been measured with high-resolution. The spectral profiles have an asymmetric shape and are fitted with a sum of two Gaussian components, broad and narrow. The central wavelengths of the two components shift toward the blue side. The flow velocities corresponding to the shifts are 4.6×10^4 m/s and 6.2×10^3 m/s in the broad and narrow components, respectively. The half widths of the broad and narrow components are equal to the Doppler widths of deuterium atoms at the temperatures of 19.6 eV and 3.5 eV, respectively. The narrow component is due to the emission from dissociated atoms and the broad component corresponds to the emission from reflected and charge exchanged atoms. The shift of the central wavelength of the broad component is caused by the emission from reflected atoms. The estimated trajectory of the reflected deuterium atoms by the limiter surface is consistent with the measured Doppler shift of the broad component. A good agreement is obtained between the calculated footprint of the magnetic field line on the limiter surface and the intensity distribution of the broad component. In addition, higher intensity of the broad component is observed around the strike point of the divertor legs. It is our expectation that magnetic structure of Heliotron J satisfies the helical divertor configuration.

References

[1] U. Samm, P. Bogenet, et al., J. Nucl. Mater. 162–164 (1989) 24.
[2] D. Reiter, P. Bogen, U. Samm, J. Nucl. Mater. 196–198 (1992) 1059.

[3] A. Kumagai, H. Kubo, H. Takenaga, et al., Plasma Phys. Control. Fusion 42 (2000) 529.
[4] D.P. Stotler, C.H. Skinner, C.F.F. Karney, Rev. Sci. Instrum. 70 (1999) 347.
[5] A. Escarguel et al., Plasma Phys. Control. Fusion 43 (2001) 1733.
[6] H. Kawazome, K. Kondo, K. Ida, K. Takiyama, et al., J. Nucl. Mater. 313–316 (2003) 716.
[7] T. Obiki, T. Mizuuchi, K. Nagasaki, et al., Nucl. Fusion 41 (2001) 833.
[8] T. Mizuuchi, M. Nakasuga, F. Sano, et al., Nucl. Mater. 290–293 (2001) 678.
[9] W.L. Ang, T. Mizuuchi, M. Nakasuga, et al., J. Plasma Res. SERIES 5 (2002) 292.
[10] T. Mizuuchi, W.L. Ang, Y. Nishioka, et al., Nucl. Mater. 313–316 (2003) 947.
[11] T. Obiki et al., Plasma Phys. Control. Fusion 42 (2000) 1151.
[12] P.C. Stangeby, in: D.E. Post, R. Behrisch (Eds.), Physics of Plasma–Wall Interactions in Controlled Fusion, Plenum, New York, 1985, p. 46.
[13] P.C. Stangeby, in: D.E. Post, R. Behrisch (Eds.), Physics of Plasma–Wall Interactions in Controlled Fusion, Plenum, New York, 1985, p. 55.
[14] W. Eckstein, IPP Report, IPP 9/117, 1998.
[15] R. Behrisch, W. Eckstein, in: D.E. Post, R. Behrisch (Eds.), Physics of Plasma–Wall Interactions in Controlled Fusion, Plenum, New York, 1985, p. 413.